Scale effects methodology applied to uprising jets in astrid

B Jourdy, D Guenadou, N Seiler, Alexandre Labergue, Michel Gradeck

SCALE EFFECTS METHODOLOGY APPLIED TO UPRISING JETS IN ASTRID

B.Jourdy[1,3], D.Guenadou[1], N.Seiler[2], A.Labergue[3], M.Gradeck[3]
[1] CEA Cadarache, DES/IRESNE/DTN/STCP/LTHC
[2] CEA Cadarache, DES/IRESNE/DTN/SMTA/LMAG
13115 Saint-Paul-Lez-Durance, FRANCE
[3] LEMTA, CNRS, UMR 7563
2 avenue de la Forêt de Haye, 54505 Vandœuvre-lès-Nancy cedex
benjamin.jourdy@cea.fr; david.guenadou@cea.fr; nathalie.marie@cea.fr;
alexandre.labergue@univ-lorraine.fr; michel.gradeck@univ-lorraine.fr

ABSTRACT

The CEA is involved in the development of the 4th generation of nuclear reactors, among which are the Sodium Cooled Fast Reactors (SFR). To support their design and safety, specific codes were developed and should be validated using experimental results from relevant mock-ups. Due to the complexity of building a full-sized prototype in the nuclear field, most of the experiments are performed on reduced-sized models but it may lead to scale effects. Such scale effect is under study in this paper, focusing on a critical issue in SFR reactor, which is the rising of the jet outgoing the core at low power.
On this issue, a scale effects methodology is detailed, using the SFR's reduced scale mock-up MICAS as the reference scale. To achieve that, dimensionless Navier-Stokes equations under Boussinesq's approximation are considered and the Vaschy-Buckingham theorem is applied to determine the most relevant dimensionless numbers: the densimetric Froude number. Experimental campaigns have been performed to measure velocity fields. Their analysis clearly shown dependency of mean pathway of the jet on this dimensionless number. Particularly, plotting the jet angle as a function of the normalized densimetric Froude number, a change of behaviour for a threshold value of 0.45 has been observed. This result also shows negligible effects on the jet rise of the phenomena happening before jet impingement on the Upper Core Structure (UCS).

KEYWORDS
SFR, Scale effects, Impinging jets, Buoyant jets

1. INTRODUCTION

In order to close the nuclear fuel cycle and use the wide spread uranium 238 isotope instead of the uranium 235 currently being used in Gen II and Gen III nuclear reactors, CEA is involved in the development of Gen IV sodium-cooled fast neutron reactors (SFR). As building a scale 1 experiment, for characterizing the reactor prototype behaviour, is both complex and expensive, most experiments are performed on small-scale mock-ups to assess new design options and validate associated simulation software. Due to sodium opacity and its reactivity with water, sodium experiments are very complex to carry out, even at small scale.

That is why a majority of such experiments are performed with a simulating fluid which is water, owing to its close properties to the sodium ones.

In 2015, in order to support the French experimental reactor project called ASTRID [1], the 1:6th scale mock-up MICAS was commissioned to study the thermal-hydraulics behaviours inside the upper plenum of this one. This mock-up allows investigations of different thermo-hydraulics issues as the gas entrainment at free surface [2] or the behaviour of the jets coming out from the core [3]. For this specific issue, these jets can be subjected to thermo-hydraulics oscillations at low power operation. And, after impinging the Upper Core Structure (UCS), they may raise due to buoyancy forces. This leads to temperature oscillating variations of some submerged vessel components and thermal fatigue, which impacts on the lifetime of the reactor.

This study focuses on the thermal-hydraulic behaviour of the hot impinging jets out of the core, especially on the transition from inertia-dominated to buoyancy-dominated jets. The first part briefly introduces both ASTRID prototype and MICAS mock-up, and provides details about the phenomenon under investigation. A theoretical study is also provided. Then, a description of the experiments conducted on MICAS and their experimental results are discussed. These results will be used as a reference for a later scale effect analysis by comparison with results at lower scales.

2. THE ASTRID PROTOTYPE AND MICAS MOCK-UP

2.1. General Overview

From 2011 to 2019, the CEA has been involved in the development of the 4th generation ASTRID (Advanced Sodium Technological Reactor for Industrial Demonstration) prototype [4]. This project aimed at demonstrating the technical options chosen and at giving an idea of the operating costs. Its power was 600MWe. However, even if this project has stopped in 2019, the CEA still carries on studies on sodium reactors and technologies. Especially, efforts head to build a numerical reactor, implying a strong validation of numerical codes.

The MICAS facility is a 1:6th sized mock-up representing the hot plenum of the ASTRID recator, based in the CEA Cadarache [5]. The scale was chosen to be a compromise between the overall size and the detail of the geometry of the vessel as MICAS geometry is homothetic to ASTRID's one, but some geometrical simplifications were necessary. Its dimensions are about 2.5 m in diameter and 1.7 m in height. Cut views of both ASTRID and MICAS are shown in Figure 1.

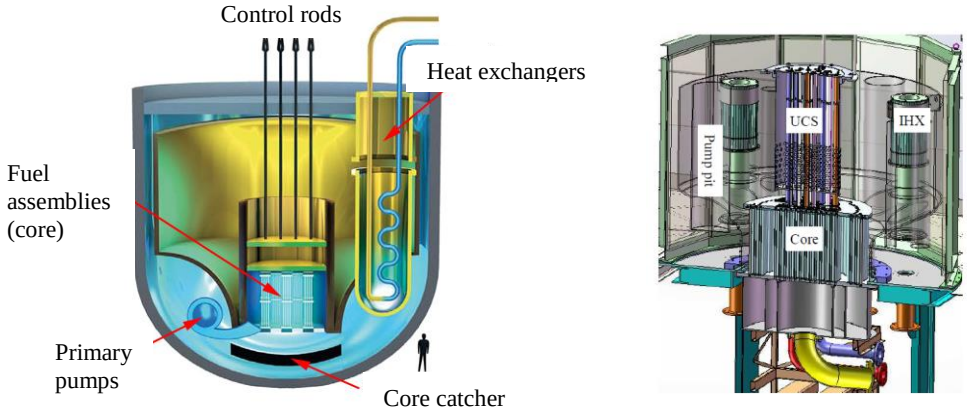

Figure 1. Cut Views of ASTRID (Left) and MICAS (Right)

2.2. Phenomenon of Interest and Problematic

Figure 2 represents a simplified schema of the flow and main components above the core. Upstream of the core, 288 hot jets are first impinging and going through a porous plate, creating loss of pressure. This porous plate deflects a small part of the flow horizontally. A part of the water (around 15% [3]) flows through the Upper Core Structure (UCS) and exit around the barrels. The bottom plate of the UCS deflects the entire part of the flow after impingement, resulting in a unique almost radial jet spreading into the upper plenum of vessel where the fluid temperature is lower than the jet's one.

At low power operating conditions, the inertia of this jet decreases and buoyancy effects become predominant, causing the jet to rise. If so, the flow pattern in the vessel is modified and leads to thermal fluctuations, causing thermal fatigue of the components of the vessel. As this phenomenon is crucial for the life expectancy of the reactor, a deep investigation is necessary.

Experimental results on MICAS are used to validate numerical codes to simulate ASTRID's thermal-hydraulics behavior. However, as we are using a downscaled mock-up to validate codes, we need to ensure that the experimental conditions are representative of the reactor ones and that the phenomenon under investigation (i.e the raise of the impinging jets) can be transposed from a scale to another without distortions. So the main point of this study is to find the most relevant dimensionless numbers to ensure the similarity of the flow, and study the dependence of the rise of the jet on these dimensionless numbers. A parameter of interest for the later scale effect's study is the critical value of this dimensionless numbers, for which the jet rises.

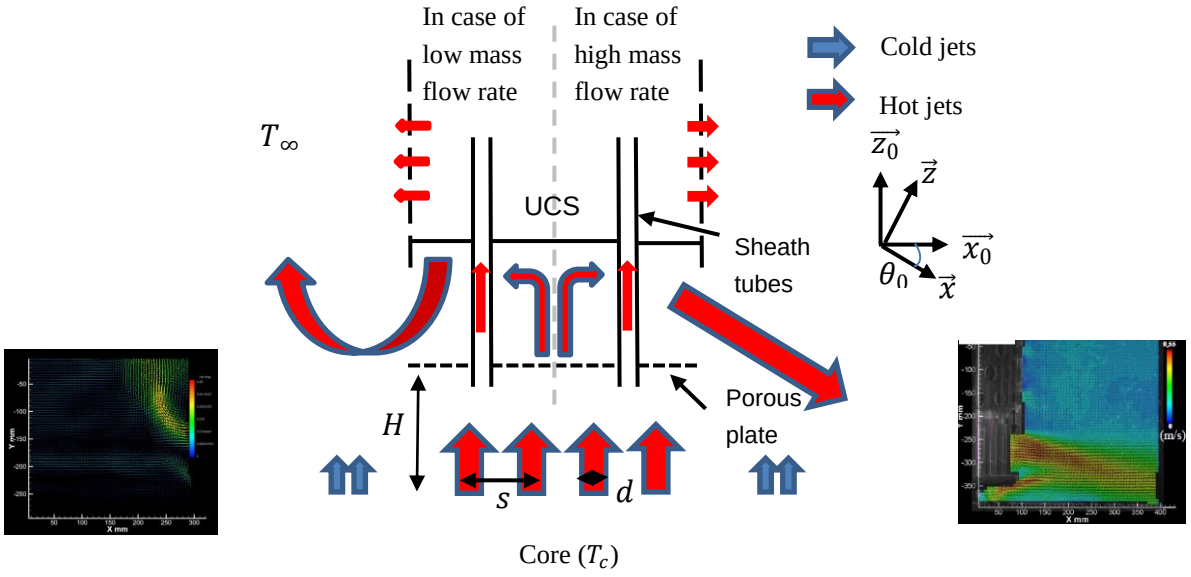

Figure 2. Schema of the flow path above the core in ASTRID and MICAS in two different cases of mass flow rate and associated experimental results (velocity vectors colored according to velocity scale)

3. THEORETICAL STUDY

3.1. Similarity of the Flow

In order to be representative of the ASTRID's flow behavior in MICAS, the Vaschy-Buckingham theorem [6] has been applied to MICAS as shown in the Table 1. This theorem allows to select dimensionless numbers whose conservation ensures the similarity of the flow between two different scales. The nomenclature is given at the end of the document. This theorem also gives geometrical dimensionless parameters such as π_1 or π_9 : these parameters do not interfere from ASTRID to MICAS as the transformation is linear from a scale to another, but can be important for the design of mock-up that need geometrical distortion.

Table 1. Dimensionless numbers obtain with Vaschy-Buckingham theorem

$\pi_1 = \frac{H}{L}$	$\pi_2 = \frac{p}{\rho . u^2} = Eu$	$\pi_3 = \frac{\eta}{\rho . u . L} = \frac{1}{Re}$
$\pi_4 = \frac{g . L}{u^2} = \frac{1}{Fr^2}$	$\pi_5 = \frac{T - T_\infty}{T_c - T_\infty}$	$\pi_6 = \beta (T_c - T_\infty)$
$\pi_7 = \frac{\alpha}{u . L} = \frac{1}{Pe}$	$\pi_8 = \frac{\rho_\infty - \rho}{\rho_\infty}$	$\pi_9 = \frac{s}{L}$

However, as the conservation of every π groups is not possible from a scale to another, we use the dimensionless governing equations known as the conservation equations in order to determine the most relevant dimensionless numbers to ensure similarity from a scale to another and calculate our experimental conditions. The study of the MICAS mock-up is divided in two different regions: first, the under-UCS zone where 288 hot jets exit the core. Then the vessel zone, where a unique jet (from the merge of the 288 core jets) is diffusing into the vessel.

Just above the core, we assume axisymmetric incompressible steady jets in cylindrical coordinates where the velocity vector u in the (r, z) coordinate system is defined by U, its axial component, and V its radial component. The notation X^* means the dimensionless variable X/X_0, X_0 being the characteristic parameter associated to the variable X. As $(\rho_\infty - \rho)/\ \rho_\infty \sim 0.2\%$, we assume the Boussinesq approximation to be valid. The scaling parameters are chosen as U_0, the average axial velocity at the jet exit, L_0 the half-width of the jet, T_c the jet's temperature out of the core and ρ_0 the jet's density at its exit out of the core. This leads to the following dimensionless conservation equations:

Mass conservation:

$$\frac{\partial U^*}{\partial z^*} + \frac{1}{r^*} \frac{\partial}{\partial r^*} (r^* V^*) = 0 \qquad (1)$$

Energy conservation:

$$\left(U^* \frac{\partial T^*}{\partial z^*} + \frac{V^*}{r^*}\frac{\partial T^*}{\partial r^*}\right) = \frac{1}{Re}\,\frac{1}{Pr}\,\frac{1}{r^*}\frac{\partial}{\partial r^*}\left(r^*\,\frac{\partial T^*}{\partial r^*}\right) \tag{2}$$

Between the porous plate and the UCS, the overall fluid temperature is homogeneous at the hot jets' temperature, around 55°C. The dimensionless momentum equation for a jet in this zone can be reduced to its axial one, as $V \ll U$, and is given by equation (3):

$$U^* \frac{\partial U^*}{\partial z^*} + V^* \frac{\partial U^*}{\partial r^*} = -\frac{1}{\rho^*}\frac{\partial Eu}{\partial z^*} + \frac{1}{Re}.\frac{1}{r^*}.\frac{\partial}{\partial r^*}\left\{r^*\,\frac{\partial U^*}{\partial r^*}\right\} \tag{3}$$

In this zone, the similarity is ensured by the conservation of the dimensionless numbers from equation (2) and (3), and the conservation of the interaction between jets. Important parameter to ensure that the dynamic interaction between the 288 jets is preserved, and thus we can consider only one single jet, are the dimensionless numbers $\pi_1$and π_9 (see Table 1) with H the nozzle-to-plate distance, d the jet diameter and s the inter-jet distance [7]. As MICAS is a linear downscaled mock-up from ASTRID, these ratios are automatically preserved. Thus, the main dimensionless numbers of interest in this zone are the Euler number and the Reynolds number. As this zone has a constant temperature, the Prandtl number is not important under the UCS.

After impingement of the UCS, the jets are merging and a single jet is spreading in the vessel. This unique jet can be studied as a planar jet in the (x_0, y_0, z_0) Cartesian system of coordinates (see Figure 2): as the axisymmetric hypothesis is still valid for planar jets, the y_0 component can be neglected.

In the vessel, the jet is not on the x_0 axis but bend with an angle θ_0 that we define as the angle between the horizontal axis x_0 and the jet axis x (see Figure 2). This angle, by convention, is positive if the jet is going downward (nominal conditions) and negative if the jet is going upward.
This definition implies the relation given equation (4):

$$\begin{cases} \vec{x} = \cos(\theta_0)\,\overrightarrow{x_0} - \sin(\theta_0)\,\overrightarrow{z_0} \\ \vec{z} = \cos(\theta_0)\,\overrightarrow{z_0} + \sin(\theta_0)\,\overrightarrow{x_0} \end{cases} \tag{4}$$

By keeping U as the axial velocity (on the x axis) and V the velocity component perpendicular to the jet's axis (on the z component), the dimensionless momentum equations on these axis become (equation (5)):

$$\begin{cases} U^* \dfrac{\partial U^*}{\partial x^*} + V^* \dfrac{\partial U^*}{\partial z^*} = \dfrac{1}{Re}\dfrac{\partial}{\partial z^*}\left\{\dfrac{\partial U^*}{\partial z^*}\right\} - \left(\dfrac{1}{Fr^2} - \dfrac{1}{Fr_D^2}\right)\sin(\theta_0) \\ U^* \dfrac{\partial V^*}{\partial x^*} + V^* \dfrac{\partial V^*}{\partial z^*} = \dfrac{1}{Re}\dfrac{\partial}{\partial z^*}\left\{\dfrac{\partial V^*}{\partial z^*}\right\} - \left(\dfrac{1}{Fr^2} - \dfrac{1}{Fr_D^2}\right)\cos(\theta_O) \end{cases} \tag{5}$$

As the flow is fully turbulent in MICAS ($Re > 10^4$), the Reynolds number may have a small influence on the jet's behavior as jets tends to be Reynolds invariant [8]. The main parameters to achieve similarity from ASTRID to MICAS (as long as the flow is fully turbulent) are the Euler's number for the jets under the UCS, and the densimetric Froude number for the jet spreading in the vessel.

This dimensionless number is defined by equation (6) where $\Delta\rho = \rho_\infty - \rho$ is the density difference between the hot jets and the surrounding environment, u is the velocity of the jet, g the gravitational constant and L the characteristic length scale of the jet.

$$Fr_D = \frac{u}{\sqrt{(\Delta\rho/\rho_\infty)\, g\, L}} \tag{6}$$

This dimensionless number is frequently used for buoyant jet studies [7] [9] [10], giving credit to its choice as a similarity parameter.

3.2. Buoyancy in Jets

For fully turbulent submerged free jets under Boussinesq's approximation, the buoyancy problem only depends on the discharge angle θ_0, and the initial jets parameters such as the flow rate Q_0, buoyancy B_0 and momentum M_0 [10]. Here, two characteristics length scales can be defined as $l_M = M_0^{3/4} / B_0^{1/2}$ and $l_Q = Q_0 / M_0^{1/2}$. l_M represents the characteristic length from momentum-driven to buoyancy-driven jet, and l_q represents the characteristic length at which the jet's exit still influence the flow.

These two characteristics length scales are related to the densimetric Froude number (equation (7)) as

$$\frac{l_Q}{l_M} = \frac{K_0}{Fr_D} \tag{7}$$

K_0 is a constant that depends of the jet's nozzle. For a round jet, $K_0 = (\pi/4)^{1/4}$. For $Fr_D \gg 1$, it has been demonstrated [10] that the geometrical parameters such as the distance from the nozzle exit to the onset of its rise X_Z as shown in Figure 2 only depends on the characteristic length scale, the densimetric Froude number and the initial discharge angle (equation (8)) :

$$\frac{Xz}{L\, Fr_D} = K(\theta_0) \tag{8}$$

In our case, the characteristic length scale is the jet diameter. $K(\theta_0)$ is a constant that only depends on the initial discharge angle. This relation shows the dependency of the jet's behaviour on the densimetric Froude number. In this study, we characterize the rise of the jet by two parameters: the distance before its raise Xz and the asymptotic angle θ_f as presented in Figure 3 below. This study will only focus on the evolution of this asymptotic angle with the densimetric Froude number.

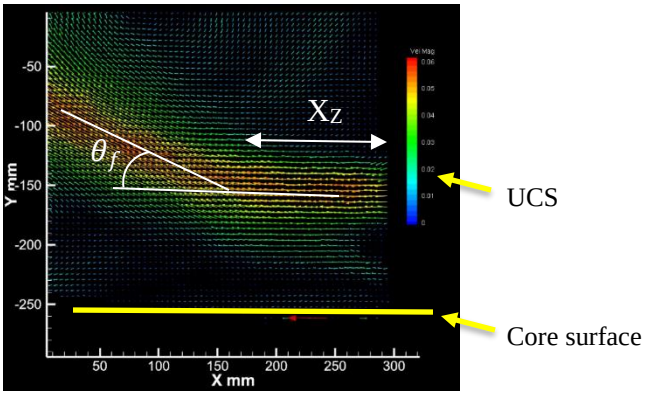

Figure 3. Characteristics features of the jet's rise

4. EXPERIMENTAL SETUP

4.1. Experimental Conditions

The inlet conditions of MICAS taken to be representative of the ASTRID reactor are calculated based to the similitude in densimetric Froude number at the core exit. The similitude in this zone allows the control of all parameters (velocity and temperature) and a relation between the jet's behaviour and the inlet conditions can then be determined. The influence of the Euler number on the behaviour of the jet will be studied later. In order to observe the rise of the jet, we decrease the inlet velocity by decreasing the mass flow and we keep the temperature differences between the jets and the environment, leading to a decrease of the densimetric Froude number with the decrease of the mass flow. The flow rate is measured with Coriolis flowmeters ($\pm 0.1\%$ of measurement range).

Most of the components in MICAS are made of optical grade transparent polymer to allow laser measurements. The maximal temperature conditions are 60°C and the minimal temperature which can be reached is around 10°C for the cold jets in the vessel. As we keep the repartition of the flow in MICAS as in ASTRID (95% of hot jets, 5% of cold ones), the operating conditions are given in Table 2. Hot jets have a temperature of 55°C and cold ones are at 10°C [5].

Table 2. Experimental conditions on MICAS compared to ASTRID's ones

	Experimental conditions	
	ASTRID (nominal)	MICAS (study range)
T_c (°C)	~570	~55
$T_c - T_\infty$ (°C)	~150	1,2 *to* 4,4
Q_c ($m^3.h^{-1}$)	~32 214	32 *to* 165
Fr_D	~ 3 *to* 27	

4.2. The Velocity Measurement Setup

The velocity fields are measured thanks to Particle Image Velocimetry (PIV) as shown Figure 4, allowing us to record 2D large velocity fields of the jets after impingement. In our setup, the laser is set on a 3-axis motion table to get a positioning as accurate as possible. Nylon particle with a density of 1000 $kg.m^{-3}$ are mixed with the water. These particles with a 4µm diameter are enlightened by the laser sheet and scatter the light. Then, their motion is recorded by a 4 Mpixels CCD camera, perpendicular to the laser sheet. Its acquisition rate is 15 Hz and results are averaged over 150 images, i.e. 10s of acquisition. PIV results averaged on a higher number of images (over 300) are giving identical results, validating the stationary nature of the flow for a 10s acquisition.

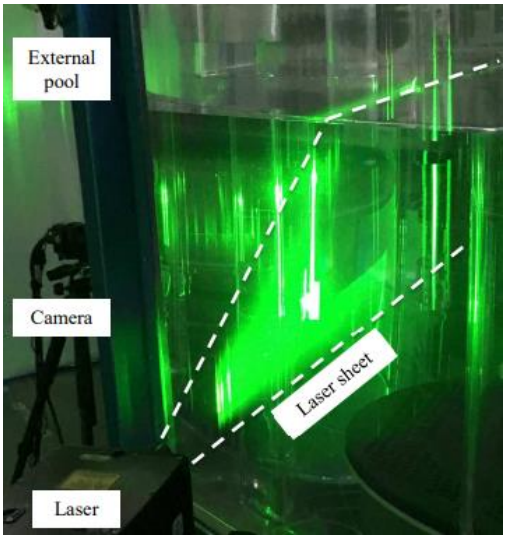

Figure 4. PIV setup on MICAS

4.3. Temperature Measurements

The inlet temperature for both hot and cold jets are measured with PT100 probes ($\pm 0.1°C$). We also put PT100 probes in the UCS to ensure that we have no thermal exchanges between the hot jets and its environment before their impingement on the UCS and spreading into the vessel.

In the vessel, we use PT100 probes to measure the ambient temperature. These probes are disposed in the middle of the vessel and next to the pump pit (green dots in the Figure 5), to measure a mixing temperature. We also use an array of thermocouples ($\pm 1°C$) to have informations about the stratification and the establishment of the flow's temperature. These 15 thermocouples are disposed on a pole with spacing of 1cm.

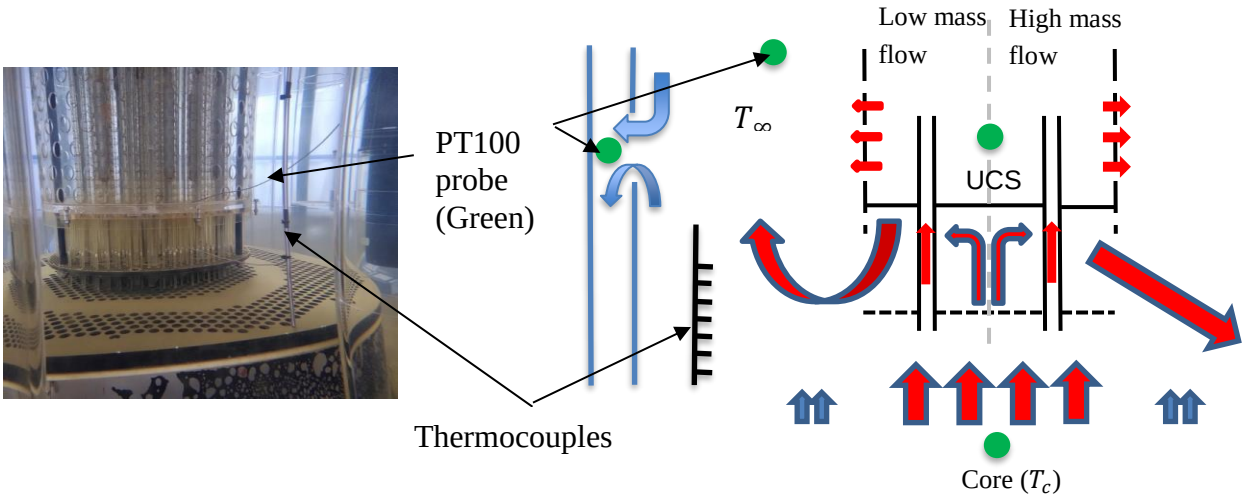

Figure 5. Temperature measurements in the vessel in MICAS

5. EXPERIMENTAL RESULTS AND COMMENTS

5.1. Velocity Measurement Results

The time-averaged PIV results show the raise of the jet in the vessel (displayed in Figure 6). For typical cases. For high mass flow rate (i.e. momentum-driven flow), we notice an initial angle around 20° (picture 1 of the Figure 6). This angle seems to be constant when buoyancy becomes unimportant and only depends on the geometry of the UCS. When the mass flow rate decrease, we notice in picture 2 of the Figure 6 that the jet start to rise and so in pictures 3 and 4, with an increasing asymptotic angle.

Because of some difficulties to achieve thermal establishment at the nominal temperature (i.e 53°C for ambient temperature and 55°C for hot jets), some results have higher temperature differences leading to a bigger asymptotic angle even if the mass flow rate is higher, as we can see in pictures 3 and 4 on the Figure 6.

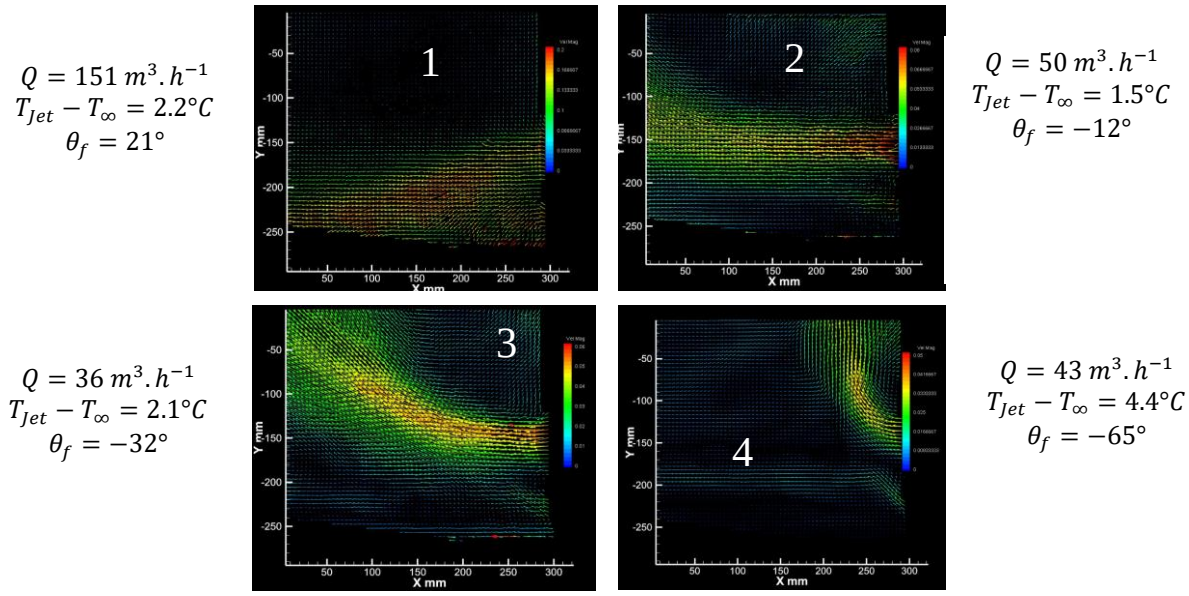

Figure 6. PIV results with decreasing mass flow

5.2. Temperature Results

As expected, the ambient temperature in the upper plenum of the vessel is subjected to thermal fluctuations. We start measurements when the flow is stabilized, i.e. when the temperature in the vessel is fluctuating around its mean value as shown Figure 7. When the flow is steady, we process to PIV measurements. The fluctuations around the mean value in the vessel are increasing with the mass flow. Maximum fluctuations observed go up to $0.4°C$ around the mean value for $Q = 151\ m^3.h^{-1}$ (see the Figure 7).

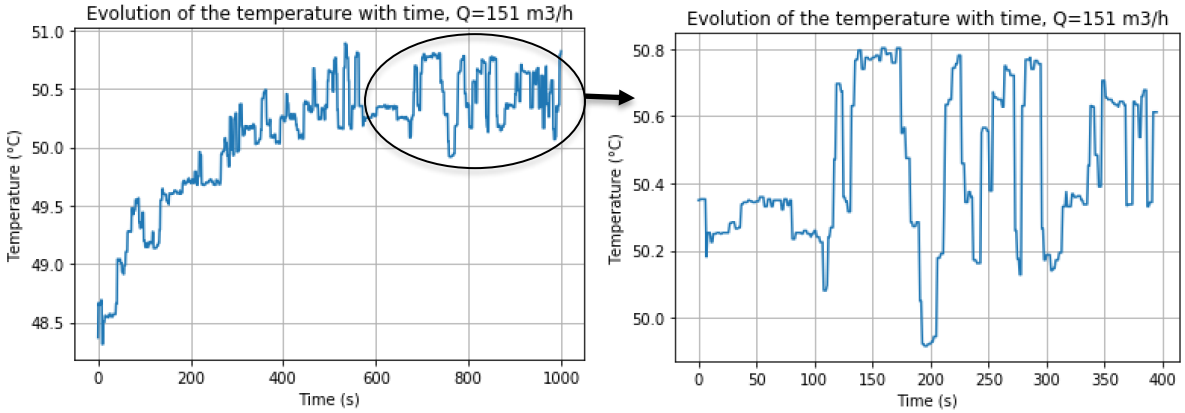

Figure 7. Stabilization of the temperature in the vessel with time for Q = 151 m^3/h measured with PT100 probe

5.3. Angle of the Jet

5.3.1. Determination of the jet's angle

We define the asymptotic angle of the jet by the angle between horizontal (referred as 0°) and jet centreline at the point where the jet start to rise. The asymptotic angle is calculated by plotting the maximum velocity magnitudes in the jet (representing the jet centreline), and defining a window in which we make a linear regression on these maximal magnitudes. This window is user-defined, meaning that it can differ from a test to another: a wrongly- positioned window could lead to aberrant points and modify the calculated angle. Hence, the window dimensions only needs to catch the jet centreline.

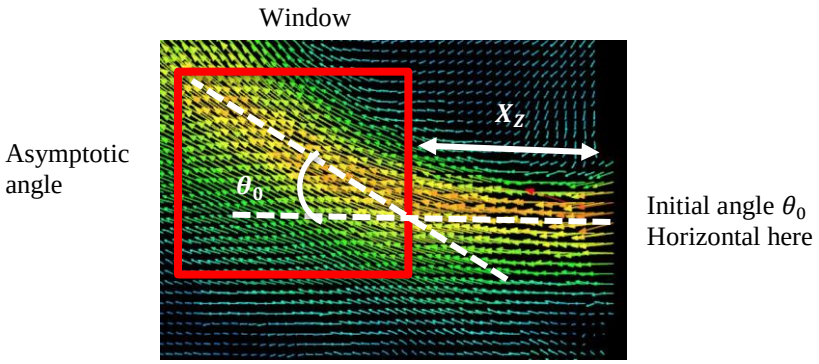

Figure 8. Calculation of the asymptotic angle

5.3.2. Asymptotic angle results

In order to show the jet's behaviour dependency on the densimetric Froude number, we plot the evolution of the asymptotic angle with this dimensionless number. The densimetric Froude number is calculated in two different zones: in the entrance of the vessel after impingement of the UCS, and at the core's exit. In

the vessel, equations (5) and (8) shown a dependency of the jet's behaviour only on the densimetric Froude number, result we want to confirm in our experiment. But, as we only control inlet conditions out of the core, we need to study the evolution of this angle with the densimetric Froude number calculated with our inlet conditions. In this zone, the jet's behaviour is supposed to be dependent on the Euler number as shown by equation (3), before diffusing in the vessel and be dependent on the densimetric Froude number.

First, we want to ensure that the behaviour of the free submerged jet in the vessel only depends on the densimetric Froude number. To do so, we calculate the experimental densimetric Froude number regarding the vessel features: the characteristic length is the planar jet's exit, calculated thanks to PIV results. The velocity is an output velocity, i.e. an average of the velocity vectors on the jet exit (equation (9)). The density differences are given thanks to the PT100 probes' measurements and tabulated values of density's evolution with temperature.

$$u_{Vessel} = \frac{1}{n_{vec}} \sum u_i \tag{9}$$

Figure 9 shows that the evolution of θ_f seems to be linear with the Fr_D on a range from 0.5 to 4.7, beyond which the angle becomes constant (between 17° and 21°). After this threshold value of $Fr_D = 4.7$, buoyancy effects become negligible and the jet behave like a momentum-driven jet only.
This saturation may depends on the UCS geometry, hypothesis that will be studied later. A regression on the linear zone gives a critical densimetric Froude number of 2.5, defined as the transition from positive to negative angle. This figure shows the dependence on the angle with the densimetric Froude number as expected by equations (5) and (8).

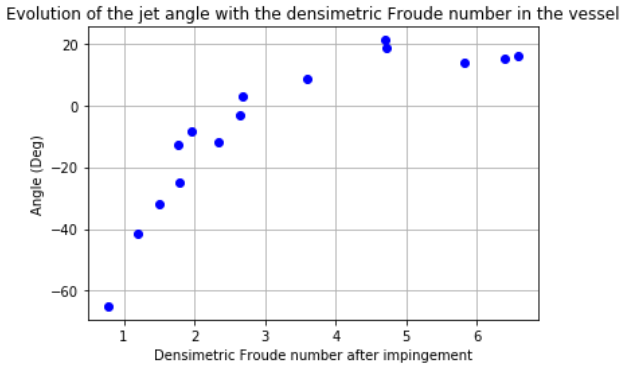

Figure 9. Evolution of the asymptotic angle with the densimetric Froude number in the upper plenum of the vessel

Figure 10 represents the evolution of the asymptotic angle θ_f with the initial densimetric Froude number Fr_D using as parameters the inlet conditions at the exit of the core. This Fr_D is calculated with the same differences of density as previously (the jet's and ambient temperature being respectively the same in both cases), but the characteristic length is the diameter of the jets in the core, and the velocity is an averaged velocity of the jets given equation (10).

$$u_{Core} = \frac{Q}{n_{jet}\, S_{jet}} \tag{10}$$

The evolution of θ_f seems again to be linear with the Fr_D on a range from 3 to 17 before reaching the asymptotic value around 20°. Buoyancy become negligible for $Fr_D = 17$. A regression on the linear zone give a critical densimetric Froude number of 9.5.

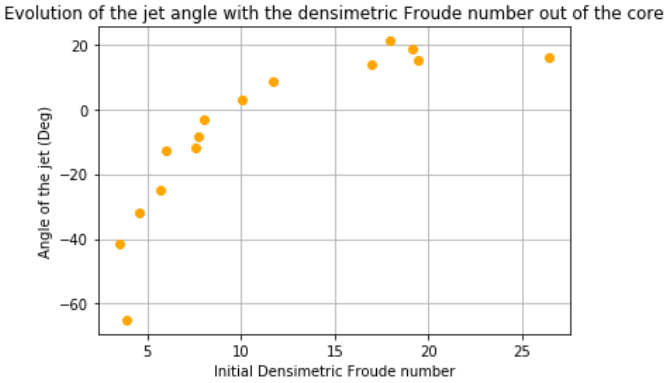

Figure 10. Evolution of the asymptotic angle with the densimetric Froude number at the outlet of the core

As the jets undergo non-linear phenomena such as loss of pressure induced by the porous plate, deviation from the barrels or impingement on the UCS, the evolution of the asymptotic angle was not expected to be similar to the evolution observed in Figure 9. To enlighten the differences due to non-linear phenomena happening between the core and the UCS, we normalize these results with the densimetric Froude number obtained at nominal mass flow in both cases.

Figure 11 gather the experimental data from Figure 9 and Figure 10 normalized by the densimetric Froude number at nominal mass flow rate. This figure shows that the results from both experiments are identical, leading to the conclusion that the non-linear phenomena have no influence on the raise of the jet in the upper plenum at MICAS's scale.

The normalized critical densimetric Froude number for which the jet's angle is $\theta_f = 0°$ is $Fr_D = 0.45$. The transition from buoyant to momentum-driven jet is reached for $Fr_D = 0.75$.

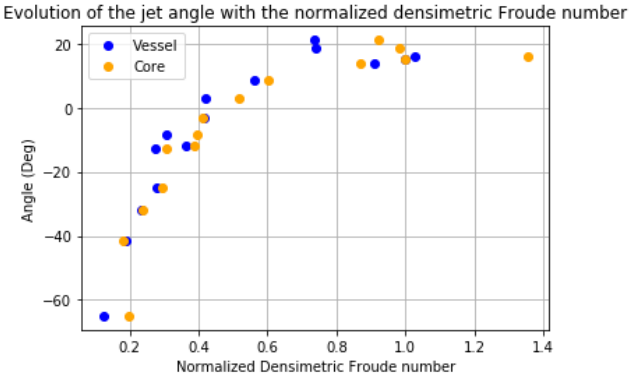

Figure 11. Evolution of the asymptotic angle with the normalized densimetric Froude number

6. CONCLUSIONS

In order to be representative of the flow in ASTRID, experimental inlet conditions on the 1:6 scaled mock-up MICAS are derived from densimetric Froude number conservation, applied to the inlet conditions out of the core. The phenomenon under study being the rise of a hot jet in a colder environment, experiments have been conducted in MICAS to characterize this phenomenon. Theoretical study imply that the behavior of the jet depends on the Euler number under the UCS and on the densimetric Froude number in the vessel. Thanks to PIV measurements for velocities and jet's angle, and temperature measurements thanks to PT100 probes, we have been able to plot the evolution of the asymptotic angle with the densimetric Froude number. This number has been calculated in two different zones, i.e. out of the core and in the vessel after impingement of the UCS. In both cases, the evolution of the asymptotic angle seems to be linear with the densimetric Froude number until the jet become momentum-dominated only. When buoyancy effects become negligible, the jet's angle has a constant value around 20°, that is assumed to be dependent on the mock-up geometry. Differences were expected between these two results, as non-linear phenomena appear between the exit of the core and the spreading in the vessel. But normalized results shown that these non-linear phenomena were negligible on the evolution of the asymptotic angle. This result imply that the Euler number has negligible effects on the rise of the jet. The critical normalized densimetric Froude number for which we consider that the jet rises has a value of 0.45. A comparison of this result with the critical densimetric Froude number at other scales will provide information about scale effects on this phenomenon.

NOMENCLATURE

d	Jets diameter $[m]$
g	Gravity $[m.s^{-2}]$
g'	Reduced gravity $[m.s^{-2}]$
n_{jet}	Number of jets
n_{vec}	Number of vectors
p	Static pressure $[Pa]$
r	Radial jet coordinate
s	Inter-jets distance $[m]$
u	Velocity $[m.s^{-1}]$
x	Planar jet axial coordinate
x_0	Horizontal coordinate
z	Planar jet coordinate perpendicular to the axial coordinate x
z_0	Vertical coordinate

α	Thermal diffusivity coefficient $[m^2.s^{-1}]$
β	Thermal expansion coefficient $[K^{-1}]$
ρ	Density of the jets $[kg.m^{-3}]$
η	Dynamic viscosity $[kg.m^{-1}.s^{-1}]$
θ	Angle of the jet with the horizontal $[deg]$

Subscripts:

∞	Ambient environment
c	Core
f	Final / Asymptotic condition
0	Initial condition

H	Nozzle-to-plate distance $[m]$
K	Constant
Q	Mass flow $[m^3.s^{-1}]$
S_{jet}	Exit surface of a jet $[m]$
T	Temperature $[°C]$
U	Axial velocity $[m.s^{-1}]$
V	Radial velocity $[m.s^{-1}]$
L	Characteristic length scale $[m]$
X_Z	Distance from the jet's exit to its raise $[m]$

Acronyms:

ASTRID:	**A**dvanced **S**odium **T**echnological **R**eactor for **I**ndustrial **D**emonstration
CEA:	**C**ommissariat aux **E**nergies **A**tomiques et aux **E**nergies **A**lternatives
IHX:	**I**nternal **H**eat E**x**changer
MICAS:	**M**aquette **I**nstrumentée du **C**ollecteur **C**haud d'**AS**TRID
SFR:	**S**odium **F**ast **R**eactors
UCS:	**U**pper **C**ore **S**tructure

Eu	Euler number
Fr	Froude number
Fr_D	Densimetric Froude number
Pe	Peclet number
Pr	Prandtl number
Re	Reynolds number

ACKNOWLEDGMENTS

The authors acknowledge the support from the CEA and its collaboration with the Lorraine University, especially the Energy & Theoretical and Applied Mechanics Laboratory. The authors also acknowledge the team of the PLATEAU platform for their support during the experimental campaigns.

REFERENCES

1. M. Saez, J. C. Robin, B. Riou, A. Villedieu, D. Deprest, and G. Prele, "Status of ASTRID nuclear island pre-conceptual design", *Proceedings of Fast Reactors and Related Fuel Cycles: Safe Technologies and Sustainable Scenarios (FR13)*, Paris, France, March 4-7 (2013).
2. D. Guenadou, P. Aubert, and J.-P. Descamps, "Analysis of the Gas Entrainment by Vortex in the Upper Plenum of the ASTRID Reactor Mock-up", *Proceedings of 12th International Topical Meeting on Nuclear Reactor Thermal Hydraulics, Operations and Safety (NUTHOS-12)*, Qindao, China, October 14-18 (2018).
3. D. Guenadou, P. Aubert, V. Biscay, and J.-P. Descamps, "Flow analysis in the upper plenum of the micas model in support of the astrid reactor program", *Proceedings of 17th International Topical Meeting on Nuclear Reactor Thermal hydraulics (NURETH-17)*, Xi'An, China (2017).
4. D. Tenchine, "Some thermal hydraulic challenges in sodium cooled fast reactors", *Nuclear Engineering and Design*, **vol. 240**(5), pp. 1195–1217 (2010).
5. D. Guenadou, I. Tkatshenko, and P. Aubert, "Plateau Facility in Support to ASTRID and the SFR Program: an Overview of the First Mock-up of the ASTRID Upper Plenum, MICAS", *Proceedings of 16th International Topical Meeting on Nuclear Reactor Thermal hydraulics (NURETH-16)*, Chicago, IL, August 30-September 4 (2015).
6. J. F. Debongnie, "Sur le Théorème de Vaschy-Buckingham", Report LMF/D53. http://hdl.handle.net/2268/197814 (2016).
7. A. C. H. Lai and J. H. W. Lee, "Dynamic Interaction of Multiple Buoyant Jets", *Journal of Fluid Mechanics*, **vol. 708**, pp. 539–575, (2012).
8. V. Heller, "Self-Similarity and Reynolds Number Invariance in Froude Modelling", *Journal of Hydraulic Research*, **vol. 55** (3), pp. 293–309, (2017).
9. M. S. Hossain and W. Rodi, *The Science & Applications of Heat and Mass Transfer: Reports, Reviews & Computer Programs, Volume 6:Turbulent Buoyant Jets and Plumes*, pp. 121–178, Elsevier, Karlsruhe, Germany (1982).
10. I. G. Papakonstantis, G. C. Christodoulou, and P. N. Papanicolaou, "Inclined Negatively Buoyant Jets 1: Geometrical Characteristics", *Journal of Hydraulic Research*, **vol. 49** (1), pp. 3–12, (2011).